

ANL/TD/CP-89770

CONF- 960690--3

Fast neutron transmission spectroscopy for illicit substance detection

T. J. Yule, B. J. Micklich, C. L. Fink, and L. Sagalovsky

Technology Development Division
Argonne National Laboratory
9700 South Cass Avenue, Argonne, IL 60439 USA

ABSTRACT

Fast-Neutron Transmission Spectroscopy (FNTS) is being investigated for detection of explosives in luggage or other small containers. This technique uses an accelerator to generate nanosecond-pulsed deuteron beams that strike a target, producing a white source of neutrons. Elemental distributions along projections through the interrogated object are obtained by analyzing neutron transmission data. Tomographic reconstruction is used to determine the spatial variations of individual elemental densities. Elemental densities are combined in a detection algorithm that indicates the presence or absence of explosives. The elemental unfolding and tomographic reconstruction algorithms have been validated by application to experimental data. System studies have been performed to study the operational characteristics and limitations of a FNTS system, and to determine the system's sensitivity to several important parameters such as flight path length and the position of the interrogated object.

1. INTRODUCTION

Fast-Neutron Transmission Spectroscopy (FNTS) is being studied for the detection of explosives in luggage and cargo containers. Fast-neutron techniques are attractive because they offer the possibility of determining the densities of light elements such as carbon, nitrogen, and oxygen within individual volume elements. Explosives are composed primarily of these elements, but are relatively rich in nitrogen and oxygen and relatively poor in carbon compared to most benign substances likely to be found in luggage or cargo. The FNTS technique was first examined¹ for bulk material analysis, and is best suited for examination of luggage or small containers having an average transmission ratio greater than about 0.01. Standard time-of-flight techniques are used to measure the energy spectrum of neutrons emitted from a collimated continuum source before and after transmission through an interrogated sample. The transmission spectrum depends on the integrated density of the elements present in the line-of-sight from the neutron source to the detector and on the total cross sections of those elements. The individual elemental areal densities (atoms per cm^2) are obtained by a linear least-squares unfolding of the transmission spectrum using the total cross sections for the elements of interest.²

2. ELEMENT UNFOLDING OF EXPERIMENTAL DATA

A key test of the elemental unfolding algorithm is its ability to unfold elemental densities from real experimental data. Experimental transmission data were provided by a group at the University of Oregon.³ The transmission-derived cross sections⁴ used in the unfolding were calculated using the radiation transport code MCNP⁵ for a $^9\text{Be}(\text{d},\text{n})$ source at $E_{\text{d}} = 4.2 \text{ MeV}$ ⁶ and a 4-m flight path with the sample located midway between source and detector (these parameter values correspond to the experimental conditions).

Unfolded areal densities for H, C, N, and O are given in Table 1 for five of the 58 items studied. We see very good agreement between the areal densities obtained by Oregon using experimentally determined cross sections and the results of the present analysis using transmission-derived cross sections calculated with MCNP. Differences in the attenuation curves are due mainly to the fact that the transmission-derived cross sections have sharper peaks and dips compared to the cross sections used by the Oregon group. The good agreement seen between the experimental attenuation data and the unfolding results confirms the validity of the elemental unfolding algorithm and the use of transmission-derived cross sections for unfolding experimental data.

MASTER

DISTRIBUTION OF THIS DOCUMENT IS UNLIMITED *PLC*

The submitted manuscript has been authored by a contractor of the U.S. Government under contract No. W-31-109-ENG-38. Accordingly, the U.S. Government retains a nonexclusive, royalty-free license to publish or reproduce the published form of this contribution, or allow others to do so, for U.S. Government purposes.

Table 1. Elemental areal densities obtained by unfolding experimental neutron transmission data.

	cotton		wool		peanut butter		book		gunpowder	
	ANL	Oregon	ANL	Oregon	ANL	Oregon	ANL	Oregon	ANL	Oregon
H	.0613	.0639	.0500	.0528	.4284	.423	.0421	.0422	.0878	.0863
C	.0307	.0305	.0331	.0313	.2326	.220	.0334	.0317	.0519	.0499
N	-.0007	.00004	.0081	.0084	.0057	.0135	-.0042	-.00197	.0224	.0260
O	.0283	.0284	.0139	.0138	.0597	.0639	.0242	.0241	.0908	.0930

3. IMAGE RECONSTRUCTION AND EXPLOSIVE DETECTION

Projection data are used in a tomographic reconstruction algorithm to determine the elemental density distributions for each element within a slice. These elemental density distributions are used to calculate an explosive signature. We are currently using a maximum likelihood algorithm for reconstruction, and a quantity termed the equivalent explosive density (EX) for an explosive signature. The details of these processes have been reported previously.^{7,8} Here we discuss the application of our image reconstruction and explosive detection routines to multiview experimental data acquired by the University of Oregon in their transmission time-of-flight experiments. A suitcase was randomly chosen from a group of lost luggage and a quantity of C-4 explosive was placed inside. The exact size and position of the explosive was unknown. The transmission measurements collected data using a linear array of sixteen detectors that viewed a slice through the suitcase. The suitcase was scanned by varying its elevation. Four scan angles of 0, 45, 90, and 135 degrees were used. The size of each detector is nominally 2.5 inches. This translates to a pixel size of approximately 3.18-cm square at the center. The transmission data were unfolded using the algorithms described in Section 2 to obtain the H, C, N, and O areal densities.

Our tomographic reconstruction programs were modified to handle fan-beam geometries. We reconstructed this projection data using a pixel resolution of 3.0 cm. Each voxel in the reconstructed slice thus represents a 3-cm cube. The suitcase was only roughly centered about the projection angle pivot point. This did not appear to have a large effect on the resulting reconstructions. In general, the measured densities are low and suggest that this suitcase was relatively lightly packed. Figure 1 shows the equivalent explosive density for various elevations. The size of each slice is 48 cm by 48 cm. The number above the reconstruction is the elevation number. Here 109 corresponds to the middle of the suitcase, and 102 corresponds to the bottom. The presence of an explosive near the bottom of the image is easily seen. The data show that the explosive size is approximately 9 to 10 cm high (approximately three slices) and approximately 6 cm (2 pixels) square. Note that the equivalent explosive density from other regions and slices is relatively small. Thus for suitcases with this packing density, the false-positive frequency should be low for large bulk explosives. Thinner explosives might require lower explosive density thresholds and could increase the false positive rate.

4. SYSTEM STUDIES

System studies are useful for exploring the range of parameters over which a FNTS system gives good results, and as an aid in designing a system to be less sensitive to small changes in parameter values. Previous studies have looked at the effect on system performance of changes in the incident particle energy and the flight path length.⁹ Here we report on the effects of sample position for $E_d = 4.2$ MeV and a 3-m flight path length. Transmission simulations were performed using a simulated fan-beam geometry and RDX samples between two and twenty cm thick. Transmission-derived cross sections used in element unfolding were determined with the same geometry and source spectrum and with samples having energy-averaged transmissions of about 0.3.

The unfolding results for HCNO areal densities are shown in Figure 2(a). The 1.5-m position corresponds to the sample being midway between source and detector. The fidelity of the unfolding results is decreased for thicker samples located nearer to the detectors, which corresponds to the greatest contribution of scattered neutrons. Thus determining cross sections for sample locations nearer the detectors does not automatically result in accurate unfolding results. Figure 2(b) shows that the best results are obtained for RDX samples having thicknesses between 5 and 10 cm. These thicknesses correspond to transmissions in the range of 15-30%, or roughly the transmission of the

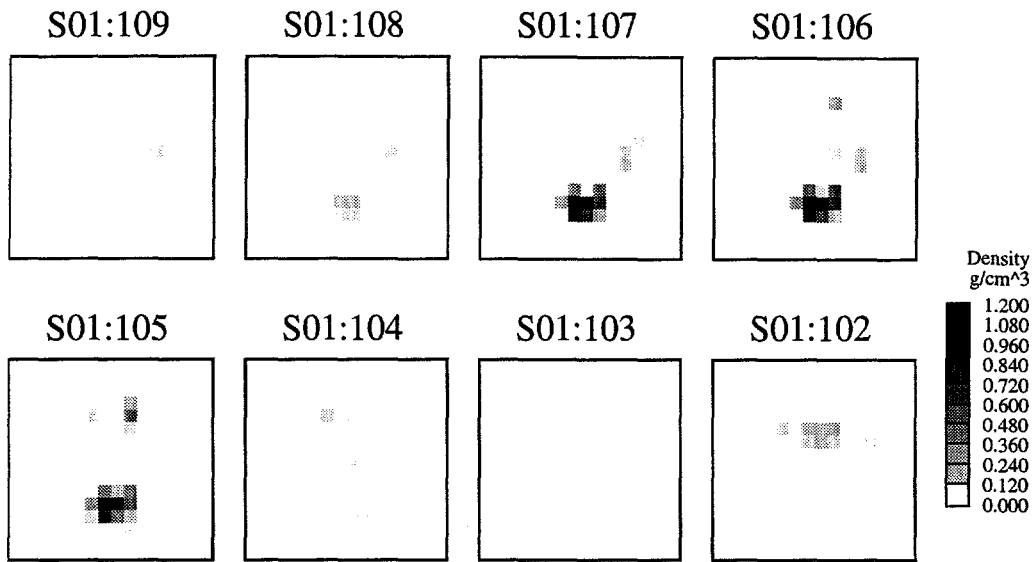


Figure 1. Equivalent explosive density vs. position for the Oregon suitcase. Pixels are approximately 3 cm square.

elemental samples used in the cross section determination. Considering all of these cases, however, we see that the unfolding algorithm yields results which are often within $\pm 5\%$ of the exact values, and outside of $\pm 10\%$ only at the extremes of the data (for very thick or very thin samples). These results are probably good enough for a robust detection algorithm to detect explosives. The standard deviations (statistical uncertainties) in the unfolded areal densities are also about 5-10%, so that any systematic errors in the unfolding results are consistent with statistical variations.

Transmission simulations were performed for the standard three-body phantom⁷ at flight path lengths of three and two meters. The reconstructed data are shown in terms of equivalent explosive density in Figure 3. For the three-meter case, the explosive block is clearly visible, although at a lower equivalent explosive density (about $1.0\text{-}1.1\text{ g/cm}^3$) than seen previously for a five-meter flight path (about 1.6 g/cm^3). For the two-meter case, the explosive is

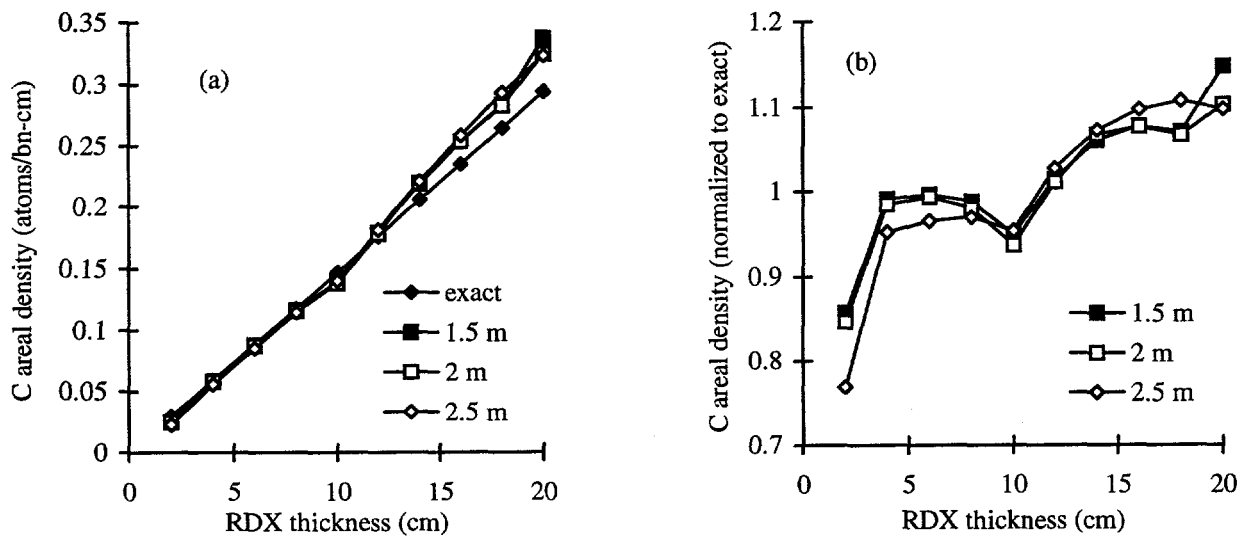
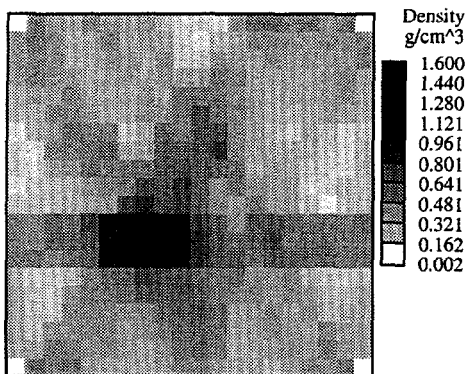


Figure 2. Carbon areal density as a function of RDX thickness and position (3-m flight path).

EX: MCNP 3-m fan beam



EX: MCNP 2-m fan beam

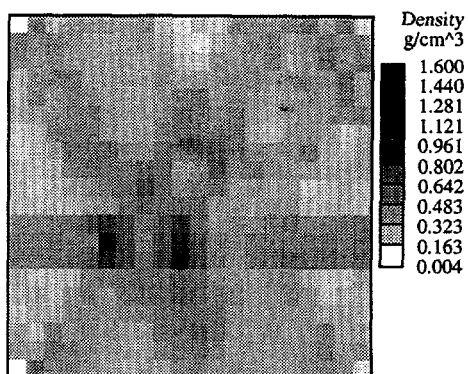


Figure 3. Equivalent explosive image for standard phantom: (a) 3-m flight path (b) 2-m flight path.

faintly visible, but at a still lower density. On the basis of these results, it appears that a three-meter flight path would be suitable for detection of bulk explosives, but detection at shorter flight paths would be more problematic.

5. CONCLUSIONS

Our element unfolding and tomographic reconstruction algorithms have been tested using experimental neutron transmission data. Element unfolding using transmission-derived cross sections gives results similar to those obtained using experimentally-measured cross sections. Tomographic reconstruction of suitcase slices for which transmission data were acquired experimentally shows that the locations of bulk explosives can be readily determined. System studies indicate that detection of bulk explosives appears feasible using flight paths of as short as three meters using fan-beam irradiation.

6. ACKNOWLEDGMENTS

This work was supported by the U.S. Federal Aviation Administration Technical Center under contract DTFA03-93-X-00021. Prof. J. C. Overley at the University of Oregon provided the experimental neutron transmission data.

7. REFERENCES

1. J. C. Overley, *J. Appl. Radiat. Isot.* **36**, 185-191 (1985); *Nucl. Instr. Meth.* **B24/25**, 1058-1062 (1987).
2. B. J. Micklich, M. K. Harper, A. H. Novick, and D. L. Smith, *Nucl. Instr. Meth.* **A353**, 646-649 (1994).
3. J. C. Overley, M. S. Chmelik, R. J. Rasmussen, R. M. S. Schofield, and H. W. Lefevre, DOT/FAA/CT-94/103 (Aug. 1994).
4. B. J. Micklich, M. K. Harper, L. Sagalovsky, and D. L. Smith, Proc. International Conference on Nuclear Data for Science and Technology, Gatlinburg, TN (May 1994).
5. J. Briesemeister, ed., LA-12625-M, Los Alamos National Laboratory (Nov. 1993).
6. J. W. Meadows, *Nucl. Instr. Meth.* **A324**, 239-246 (1993).
7. C. L. Fink, B. J. Micklich, T. J. Yule, P. Humm, L. Sagalovsky, and M. M. Martin, *Nucl. Instr. Meth.* **B99**, 748-752 (1996).
8. C. L. Fink, P. G. Humm, M. M. Martin, and B. J. Micklich, Proc. IEEE Nuclear Science Symposium, San Francisco (Oct. 1995).
9. B. J. Micklich, C. L. Fink, and L. Sagalovsky, European Symposium on Optics for Environmental and Public Safety, SPIE **2511**, 33-44, Munich, Germany (June 1995).

DISCLAIMER

This report was prepared as an account of work sponsored by an agency of the United States Government. Neither the United States Government nor any agency thereof, nor any of their employees, makes any warranty, express or implied, or assumes any legal liability or responsibility for the accuracy, completeness, or usefulness of any information, apparatus, product, or process disclosed, or represents that its use would not infringe privately owned rights. Reference herein to any specific commercial product, process, or service by trade name, trademark, manufacturer, or otherwise does not necessarily constitute or imply its endorsement, recommendation, or favoring by the United States Government or any agency thereof. The views and opinions of authors expressed herein do not necessarily state or reflect those of the United States Government or any agency thereof.

DISCLAIMER

**Portions of this document may be illegible
in electronic image products. Images are
produced from the best available original
document.**